

# Hydrothermal modelling of Takhini Hot Springs (NTS 105D/14)

*Xavier Léveillé-Dallaire\**

Institut national de la recherche scientifique

*Jasmin Raymond*

Institut national de la recherche scientifique

Léveillé-Dallaire, X. and Raymond, J., 2024. Hydrothermal modelling of Takhini Hot Springs (NTS 105D/14). In: Yukon Exploration and Geology Technical Papers 2023, L.H. Weston and Purple Rock Inc. (eds.), Yukon Geological Survey, p. 77–96.

## Abstract

The Takhini Hot Springs, located northeast of Whitehorse, Yukon, exhibits significant geothermal potential with a surface water temperature of 46°C. To address the limited geological knowledge in the region, a 500 m deep well was strategically drilled in this area and intercepted warm groundwater (25°C) at a depth of 450 m. The objective of this study was to assess the geothermal potential of the Takhini Hot Springs area using 2D subsurface flow and heat transfer simulations to numerically replicate the observed temperature and gain a better understanding of heat transfer mechanisms affecting the geothermal resource. Inclined permeable layers such as contacts between fractured sedimentary units appear to facilitate groundwater circulation, creating a path for geothermal fluids to rise. A fault that is assumed to be subvertical is present in the area but does not impact the model's water circulation. A sensitivity analysis was conducted to define the impact of each model parameter on the hot springs temperature and on temperature profiles simulated in the Takhini well. The analysis revealed that boundary conditions, including basal heat flux and surface recharge, as well as rock thermal conductivity and permeability, are the most influential parameters in the model.

## Introduction

The Yukon Territory in northwestern Canada shows substantial geothermal potential due to its proximity to the Pacific Ring of Fire, the abundance of plutonic rocks, the presence of major crustal-scale structures such as the Tintina and Denali faults, extensive sedimentary rock deposits and the existence of numerous hot springs. Studies on Curie depth (Witter et al., 2018), radiogenic heat generation potential from granitoid rocks (Colpron, 2019), and rock thermohydraulic properties (Langevin et al., 2020a), indicate that southern Yukon is expected to have the highest geothermal potential in the territory. Unfortunately, few detailed geothermal

studies have been conducted, so sparse geoscientific data are available for an in-depth understanding of the available geothermal resources. To address this data gap, the Yukon Geological Survey (YGS) launched a geothermal-focused research initiative to integrate geological, geochemical and geophysical data, and collect additional subsurface temperature data through drilling in specific geological contexts. The wells drilled as part of this initiative are instrumental in acquiring temperature gradient measurements, contributing to a more comprehensive understanding of the region's geothermal potential.

\* [xavier.leveillee-dallaire@inrs.ca](mailto:xavier.leveillee-dallaire@inrs.ca)

This paper presents an assessment of the geothermal potential of the Takhini Hot Springs area using well data acquired by YGS in 2017 from YGS-17-01, referred to here as the 'Takhini well'. Insights from regional geological investigations and rock thermohydraulic property analysis were combined to conduct finite element simulations of subsurface flow and heat transfer using the COMSOL Multiphysics software (COMSOL, 2023). Our objective was to better understand heat transfer mechanisms that facilitate warm groundwater to seep at surface. Innovative concepts supported by 2D numerical simulations of deep subsurface temperature are presented to explain the origin of the Takhini Hot Springs. The simulations aimed to identify conditions under which the geothermal gradient measured in the Takhini well can be reproduced and provide insights into the presence of 46°C groundwater at the Takhini Hot Springs by considering the thermohydraulic properties of the surrounding rock formations. Knowledge gained through this assessment can benefit renewable energy development in the Yukon with a better understanding of the geothermal potential of the area. The Takhini Hot Springs is a major tourist attraction; understanding its origin can promote sustainable development and responsible resource management.

## Project background

### Previous geothermal studies

The Government of Yukon aims to achieve a 45% reduction in greenhouse gas emissions by 2030, primarily by reductions in fossil fuel use in transportation, heating, electricity generation, and industrial activities (Government of Yukon, 2022). Geothermal energy is presented as a source of green energy as part of the government's strategy to combat climate change, although little work to date has been done to better understand the Yukon's green energy resources. The YGS geothermal research program was launched in 2016 as part of the Government of Yukon's initiative to find green energy solutions. Initial studies focused on regional assessment of geothermal potential, including potential radiogenic heat production (RHP; Colpron, 2019) and regional mapping of Curie depths (Witter et al., 2018; Fraser et al., 2019). The YGS also drilled two 500 m deep temperature gradient wells to further characterize the geothermal gradient in target areas. One of these wells (YGS-17-01), which is the focus of this paper, was drilled in the vicinity of the Takhini River,

approximately 2 km west of Takhini Hot Springs (Fig. 1). This area is adjacent to a granitoid intrusion with an average potential RHP value of 4.1  $\mu\text{W}/\text{m}^3$ , which is slightly higher than the average value of 2.5  $\mu\text{W}/\text{m}^3$  (Artemieva et al., 2017; Colpron, 2019). Drilling operations were conducted on a parcel of Settlement Land of the Ta'an Kwäch'än Council and were carried out in collaboration with the Da Daghay Development Corporation.

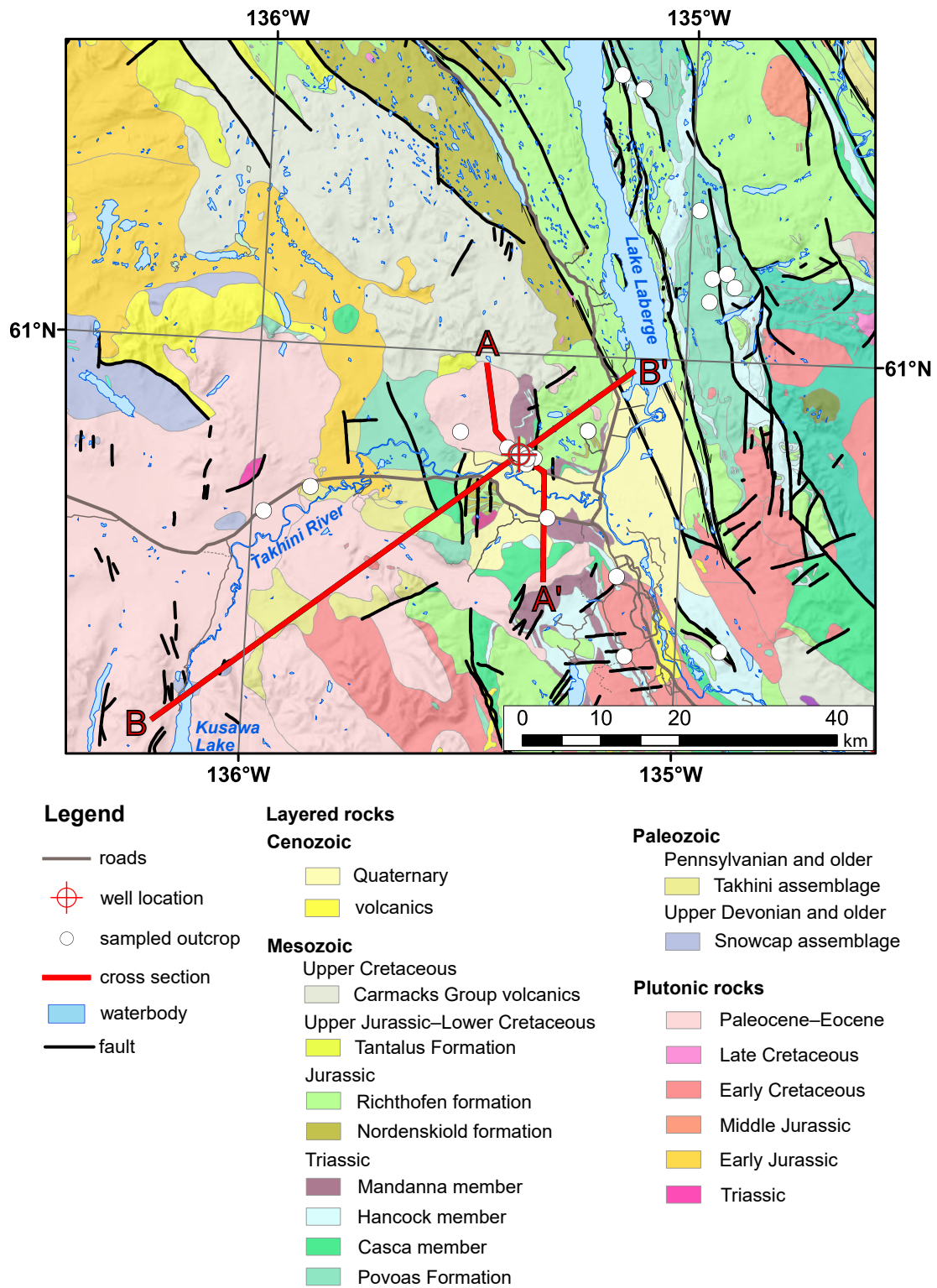
Comprehensive details and findings of the YGS' Takhini geothermal well drilling program are presented in Fraser et al. (2019). After drilling, a thermistor cable with sensors at 50 m intervals was installed in the well and temperature was measured periodically over a six-month period. After re-equilibration, the top 450 m of the well featured a geothermal gradient of 16.5°C/km, and the final 50 m showed a substantial gradient of 250°C/km (Fig. 2). This drastic gradient change is interpreted to have resulted from warm groundwater flowing along permeable rock layers.

## Geological setting

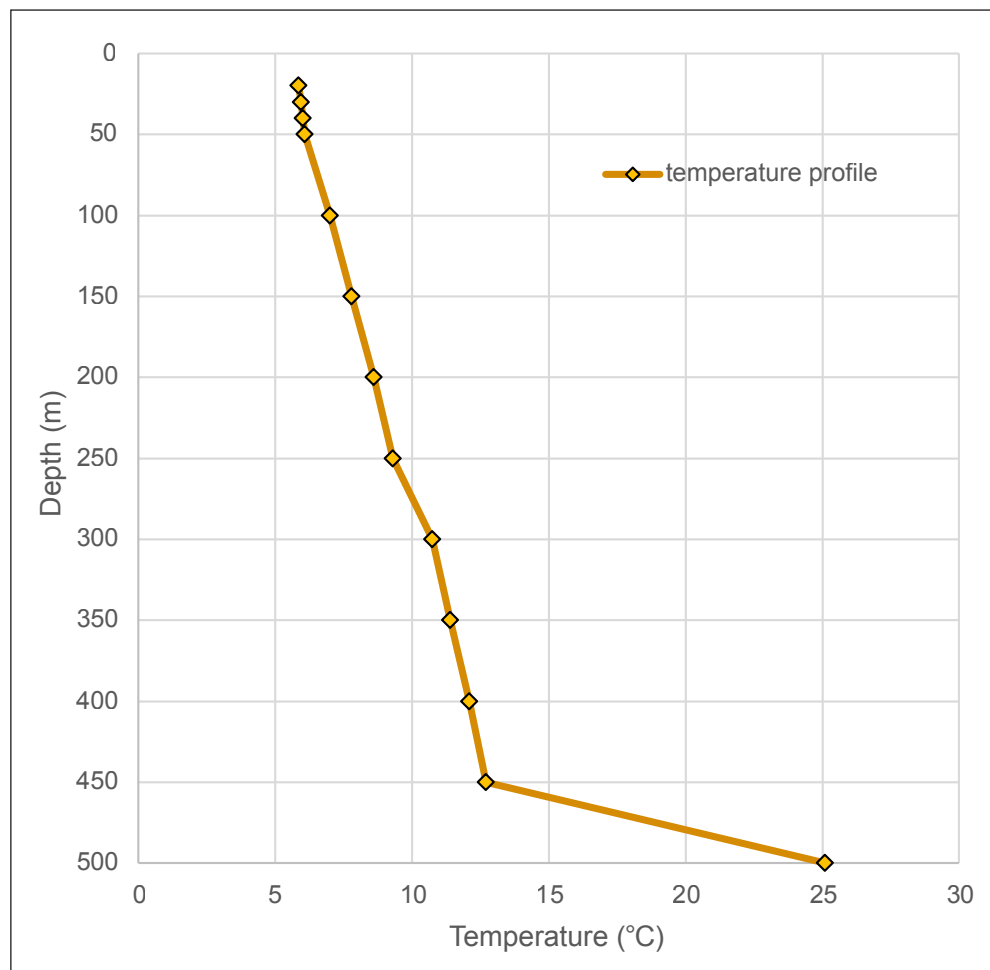
At a regional scale, the Yukon can be divided into two major geological domains: rocks of the North American continental margin, and terranes that accreted to the western margin of North America in the Mesozoic–Cenozoic (Hart, 1997; Monger and Price, 2002). These two domains are roughly separated by the northwest-striking Tintina fault, a dextral strike-slip fault with approximately 430 km of early Cenozoic displacement (Gabrielse et al., 2006).

The Whitehorse trough, where the Takhini Hot Springs occur, is a northwest-elongated sedimentary basin southwest of the Tintina fault that extends from northern British Columbia to the Yukon (Hart, 1997). The basin is characterized by Lower to Middle Jurassic sedimentary rocks of the Laberge Group that include a mixture of marine and fluvial sedimentary rocks and minor volcanic rocks (Fig. 3). Rocks of the Whitehorse trough were deposited in a synorogenic basin that overlaps Stikinia and the Cache Creek allochthonous terrane (Colpron et al., 2015, 2022).

Near the Takhini well site, rocks of the Whitehorse trough (Laberge Group) consist of marine sandstone and shale of the Richthofen formation and intercalated volcaniclastic rocks of the Nordenskiöld facies (Colpron



**Figure 1.** Geological map of the Takhini Hot Springs area showing the locations of cross sections A–A' and B–B' from Langevin et al. (2020a). Geology from Yukon Geological Survey (2022, 2023).



**Figure 2.** Downhole temperature profile measured in the Takhini well (YGS-17-01); after Fraser et al. (2019) in Langevin et al. (2020a).

et al., 2015; van Drecht et al., 2022). The Laberge Group rocks overlie the Upper Triassic siliciclastic (Casca and Mandanna members) and carbonate rocks (Hancock member) of the Lewes River Group (Hart, 1997). Middle Jurassic to Paleogene granitoid plutons intrude the Whitehorse trough and underlying terranes. Notably, an Eocene granite pluton (ca. 54 Ma; Hart, 1997) occurs approximately 2 km west of the Takhini drill site (Figs. 1, 3). To the southwest, rocks of the Takhini assemblage (upper Paleozoic volcanic rocks of Stikinia) are intruded by the Annie Ned batholith (ca. 57 Ma; Hart, 1997).

**Thermohydraulic rock properties and heat generation**

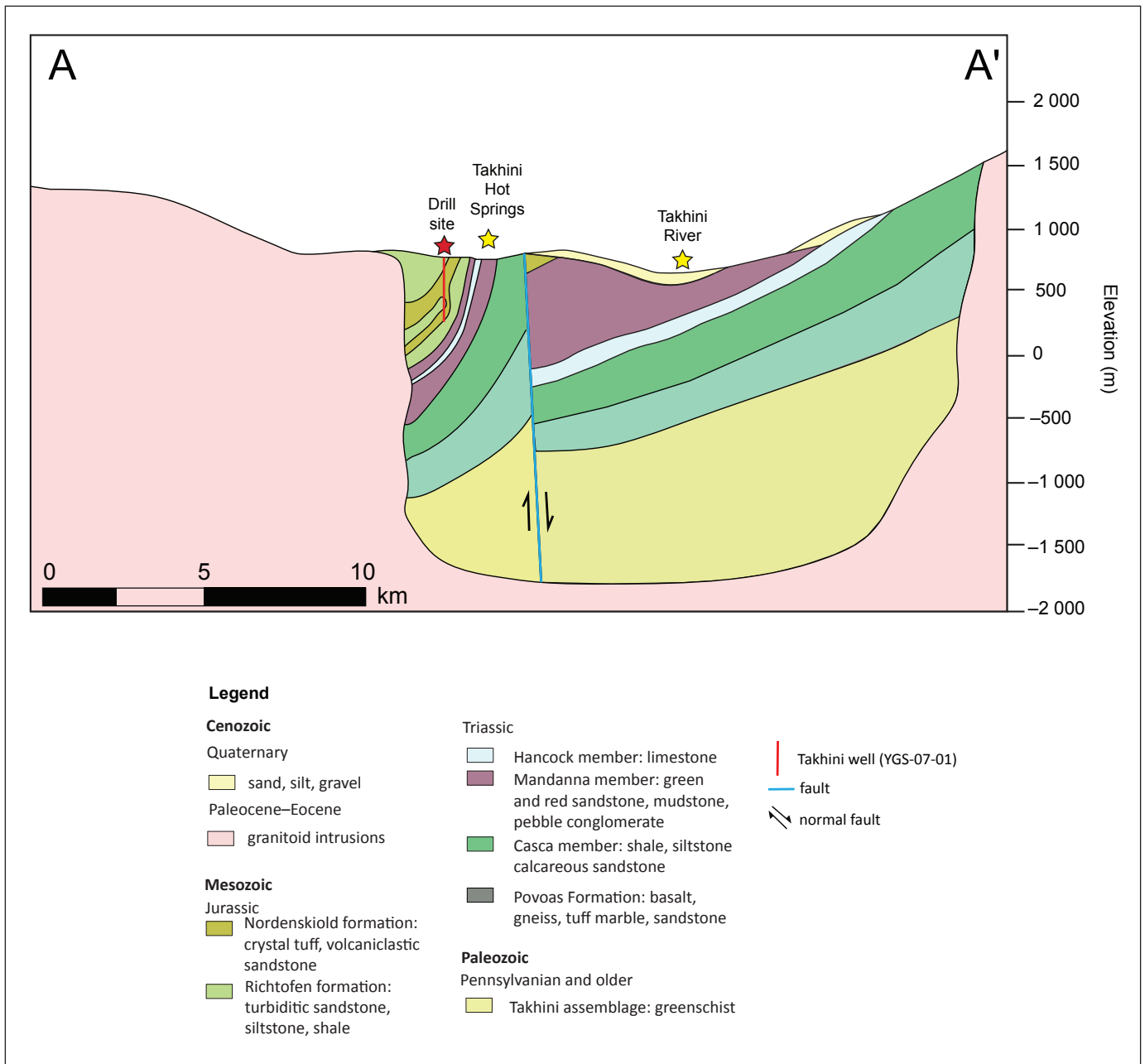
Rock thermohydraulic properties evaluated by Langevin et al. (2020a, b) were used to define the numerical model parameters in this study. Pertinent results from

these two publications are summarized here for context.

Logging of the Takhini well core was undertaken at the YGS H.S. Bostock Core Library in Whitehorse using hand samples and thin sections. Representative samples were also taken from relevant outcrops in the vicinity of the well to aid in interpretation. The Takhini well intercepted Lower Jurassic volcanoclastic rocks of the Nordenskiöld facies and marine siliciclastic strata of the Richthofen formation (Laberge Group). At surface, strata strike approximately 162 degrees north and dip approximately 75 degrees to the southwest. In the vertical wellbore, the dip angles on bedding vary from 45 to 85 degrees from horizontal. The well can be divided into six main lithostratigraphic

units, labelled A to F in Figure 4. Unit A (55.0–82.9 m depth) mainly consists of volcanoclastic sandstone, basaltic tuff and mafic dikes. Unit B (82.9–167.1 m) consists of medium and coarse-grained volcanoclastic sandstone and minor shale. Unit C (167.1–258.1 m) consists of coarser grained version of unit B, with local pervasive carbonate alteration. Unit D (258.1–347.0 m) consists of a bluish-grey, medium to very coarse grained volcanoclastic sandstone, minor siltstone, shale and brecciated fault zones. Unit E (347.0–462.5 m) is a shale unit cut by a series of mafic and felsic dikes. Unit F (462.5–500.0 m) consists of a coarse-grained volcanoclastic sandstone succession cut by an intermediate dike.

Two cross sections were constructed through the Takhini well area to gain a better understanding of the groundwater flow and heat transfer in the region

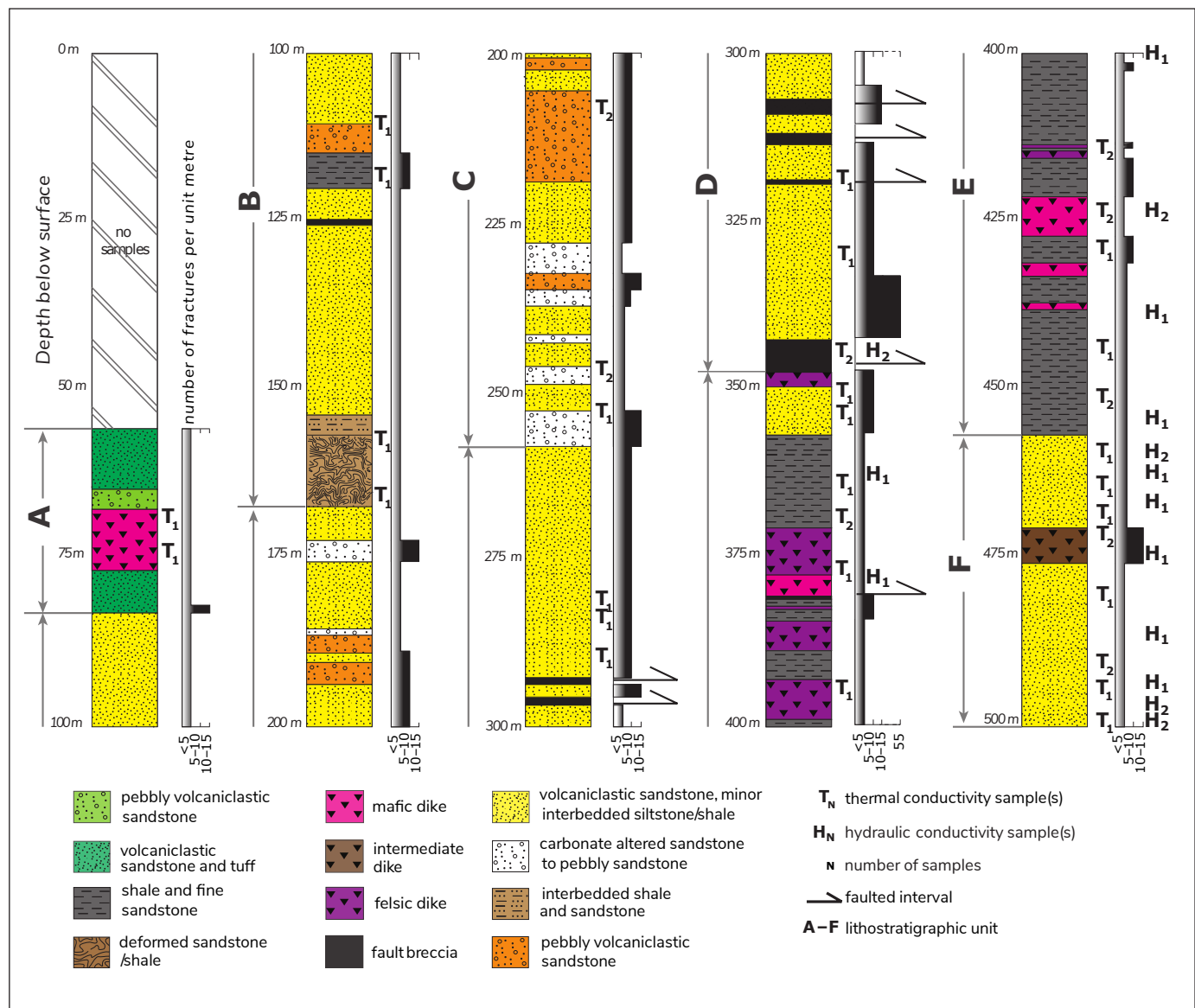


**Figure 3.** Cross section A–A' showing geological interpretations in the vicinity of the Takhini well (YGS-17-01; from Langevin et al., 2020a). Geology after Hart (1997) and Colpron et al. (2015).

(Figs. 1, 3). These cross sections were constrained using existing geological maps, core samples from the Takhini well and specific outcrop samples. Our work is based on cross section A–A' of Langevin et al. (2020a; Fig. 3), which was used to define the geometry of strata, faults, contacts and rock types in our model. Basement rocks consist of variably deformed and metamorphosed greenschist of the Takhini assemblage, unconformably overlain by Upper Triassic to Jurassic sedimentary and volcanoclastic sequences. The sedimentary rocks are cut

by steeply dipping normal faults that were developed during regional tectonic activity in the Cretaceous (Hart, 1997). Extrapolation of faults and bed thicknesses at depth are speculative.




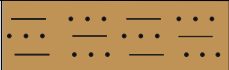








Thermohydraulic analyses were conducted on both well core and field samples. A total of 43 well samples were analyzed for thermal conductivity at the Laboratoire ouvert de géothermie at the Institut national de la recherche scientifique (INRS) in Québec City, Québec.



**Figure 4.** Lithostratigraphy of the Takhini well (YGS-17-01) including fracture density and locations of samples taken for thermal and hydraulic conductivity analyses (after Langevin et al., 2020a).

Thermal conductivity values in the well range from 0.63 to 4.19 W/(m·K) (Fig. 5). The highest average value was measured in the deformed sandstone and shale unit (3.81 W/(m·K)). The lowest average value was found in the breccia unit (0.98 W/(m·K)) ; Langevin et al., 2020a). Analysis of thermal conductivity also included three samples from the Flat Creek pluton and two samples from the Annie Ned batholith (Ruby Range suite), which yielded average values of 2.53 and 2.39 W/(m·K), respectively. The radiogenic heat production was also measured, with an average of 3.00  $\mu\text{W}/\text{m}^3$  for the Flat Creek pluton and 1.66  $\mu\text{W}/\text{m}^3$  for the Annie Ned batholith (Langevin et al., 2020b)

Hydraulic conductivity was measured on three groups of rocks: consolidated rocks (19 core and 16 outcrop samples); unconsolidated fragments of core samples; and fractured rocks (core fractures). Analyses were made using a transient gas permeameter for consolidated core plugs and outcrop samples (PPP-250; Core Lab Instruments, 2016); grain size distribution determination for unconsolidated rock fragments (Alvarado Blohm et al., 2016); and fracture aperture and spacing using the cubic law (Witherspoon et al., 1980). Measurements indicate a general hydraulic conductivity of less than  $9.6 \times 10^{-9}$  m/s for consolidated rock matrix, with a maximum of  $1.6 \times 10^{-7}$  m/s, whereas

| Lithology   | Lithology graphic   | Average thermal conductivity (W/(m · K)) | Thermal conductivity [low; high] (W/(m · K)) | Number of samples |
|---|---|--|--|-------------------|
| deformed sandstone and shale                                    |    | 3.81                                     | [3.43; 4.19]                                 | 1                 |
| carbonate altered sandstone to pebbly sandstone                 |    | 3.47                                     | [3.05; 3.89]                                 | 3                 |
| felsic dike   |    | 3.38                                     | [3.18; 3.58]                                 | 5                 |
| interbedded shale and sandstone                                 |    | 3.28                                     | [2.95; 3.61]                                 | 1                 |
| shale and fine sandstone  |    | 3.16                                     | [2.32; 4.00]                                 | 7                 |
| pebbly volcanoclastic sandstone                                 |    | 3.16                                     | [3.02; 3.30]                                 | 3                 |
| intermediate dike   |    | 3.06                                     | [3.04; 3.08]                                 | 2                 |
| volcanoclastic sandstone, minor interbedded siltstone and shale |   | 2.94                                     | [2.64; 3.24]                                 | 14                |
| mafic dike  |  | 2.39                                     | [2.15; 2.63]                                 | 5                 |
| fault breccia   |  | 0.98                                     | [0.63; 1.33]                                 | 2                 |
| pebbly volcanoclastic sandstone                                 |  | -  | -  | 0                 |
| volcanoclastic sandstone and mafic tuff                         |  | -  | -  | 0                 |

**Figure 5.** Thermal conductivity of rock formations in the Takhini well (YGS-17-01; after Langevin et al., 2020a).





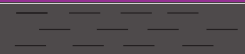


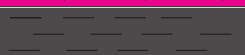
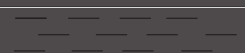
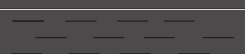











brecciated (unconsolidated) rock samples had an average hydraulic conductivity of  $5.6 \times 10^{-4}$  m/s (Fig. 6). Lithologies shown in Figure 6 correspond to the ones shown in Figures 4 and 5. Intervals of fractured rock resulted in values on the order of  $10^{-14}$  to  $10^{-10}$  m/s for superfine apertures,  $10^{-10}$  to  $10^{-6}$  m/s for fine apertures, and  $10^{-6}$  to  $10^{-1}$  m/s for moderate to large apertures.

From these studies, it was determined that the Takhini area is prone to conductive and forced convective heat transfer typical of an orogenic belt (Moeck, 2014; Langevin et al., 2020a). In these settings, forced convective heat transfer is generally found in steeply dipping crustal faults and permeable structures, which act as conduits for rising warm groundwater.

## Numerical heat transfer model

### Conceptual model and assumptions

A 2D conceptual model, simplified from the model proposed by Langevin et al. (2020a, b), is presented in Figure 7. The model has three rock types, including sedimentary rocks in the centre, the Flat Creek Eocene granite to the north and the Annie Ned batholith (granite) to the south. The model also includes four permeable layers (green lines), which represent boundaries between sedimentary units, as well as a subvertical fault (blue line). The lateral boundaries of the basin were simplified with straight vertical lines at the margin of both plutons.

| Rock type   | Lithology   | Well depth (m)        | Hydraulic conductivity (m/s) |
|---|---|-----------------------|------------------------------|
| Consolidated  |    | 302.83–303.07         | $<9.6 \times 10^{-9}$        |
|   |    | 325.16–325.34         | $<9.6 \times 10^{-9}$        |
|   |    | 363.17–363.32         | $<9.6 \times 10^{-9}$        |
|   |    | 378.89–379.09         | $<9.6 \times 10^{-9}$        |
|   |    | 401.86–402.08         | $<9.6 \times 10^{-9}$        |
|   |    | 423.03–423.18         | $<9.6 \times 10^{-9}$        |
|   |    | 424.58–424.76         | $<9.6 \times 10^{-9}$        |
|   |    | 439.86–440.00         | $1.6 \times 10^{-7}$         |
|   |    | 455.00–455.25         | $7.4 \times 10^{-8}$         |
|   |    | 459.27–459.43         | $<9.6 \times 10^{-9}$        |
|   |    | 461.44–461.59         | $<9.6 \times 10^{-9}$        |
|   |    | 462.85–463.00         | $<9.6 \times 10^{-9}$        |
|   |   | 467.00–467.15         | $<9.6 \times 10^{-9}$        |
|   |  | 475.00–475.28         | $<9.6 \times 10^{-9}$        |
|   |  | 485.95–486.10         | $<9.6 \times 10^{-9}$        |
|   |  | 493.10–493.25         | $<9.6 \times 10^{-9}$        |
|  | 496.40–496.50   | $<9.6 \times 10^{-9}$ |                              |
|  | 497.00–497.15   | $<9.6 \times 10^{-9}$ |                              |
|  | 497.84–498.00   | $<9.6 \times 10^{-9}$ |                              |
| Unconsolidated  |  | 345.32–345.52         | $1.8 \times 10^{-5}$         |
|   |  | 346.00–346.20         | $2.0 \times 10^{-5}$         |

**Figure 6.** Hydraulic conductivity of consolidated and unconsolidated rocks in the Takhini well (YGS-17-01; after Langevin et al., 2020a).

The Takhini Hot Springs are situated in sedimentary rocks between two permeable layers, approximately 2 km southeast of the Takhini well and 2 km north of the subvertical fault in the model. The Takhini well in the model intersects a permeable layer at approximately 450 m depth, aiming to recreate the Takhini well temperature gradient change with numerical simulations (Fig. 2; Fraser et al., 2019). The Takhini River is located approximately 2 km south of the subvertical fault in the model.

### Governing equations

The model was developed using the subsurface flow module available in the COMSOL Multiphysics software (COMSOL, 2023). Steady state groundwater flow was simulated using the finite element method based on Darcy’s law coupled with heat transfer in porous media, allowing us to simulate convective heat transfer, mainly occurring along permeable layers. Darcy’s law is expressed as



$$\mathbf{u} = -\frac{k}{\mu} \nabla P \quad (1)$$

where  $\mathbf{u}$  represents the fluid velocity within the porous medium in  $\text{m}^3/\text{s}$ ,  $k$  is the permeability of the medium in  $\text{m}^2$ ,  $\mu$  is the dynamic viscosity of the fluid in  $\text{kg}/(\text{m}\cdot\text{s})$ , and  $\nabla P$  represents the pressure gradient in  $\text{Pa}/\text{m}$ . Velocity vectors found with the flow solution are used to compute heat transfer according to

$$\lambda_b \left( \frac{\partial^2 T}{\partial x^2} + \frac{\partial^2 T}{\partial z^2} \right) - \rho_f c_f \left( u_x \frac{\partial T}{\partial x} + u_z \frac{\partial T}{\partial z} \right) + A = 0 \quad (2)$$

where  $\lambda_b$  is the bulk thermal conductivity in  $\text{W}/(\text{m}\cdot\text{K})$ ,  $T$  represents the temperature in  $\text{K}$ ,  $\rho_f$  is the density of the fluid in  $\text{kg}/\text{m}^3$ ,  $c_f$  is the heat capacity of the fluid in  $\text{J}/(\text{kg}\cdot\text{K})$  and  $A$  is the internal heat generation from the decay of radiogenic elements in  $\mu\text{W}/\text{m}^3$ .

## Geometry and subsurface properties

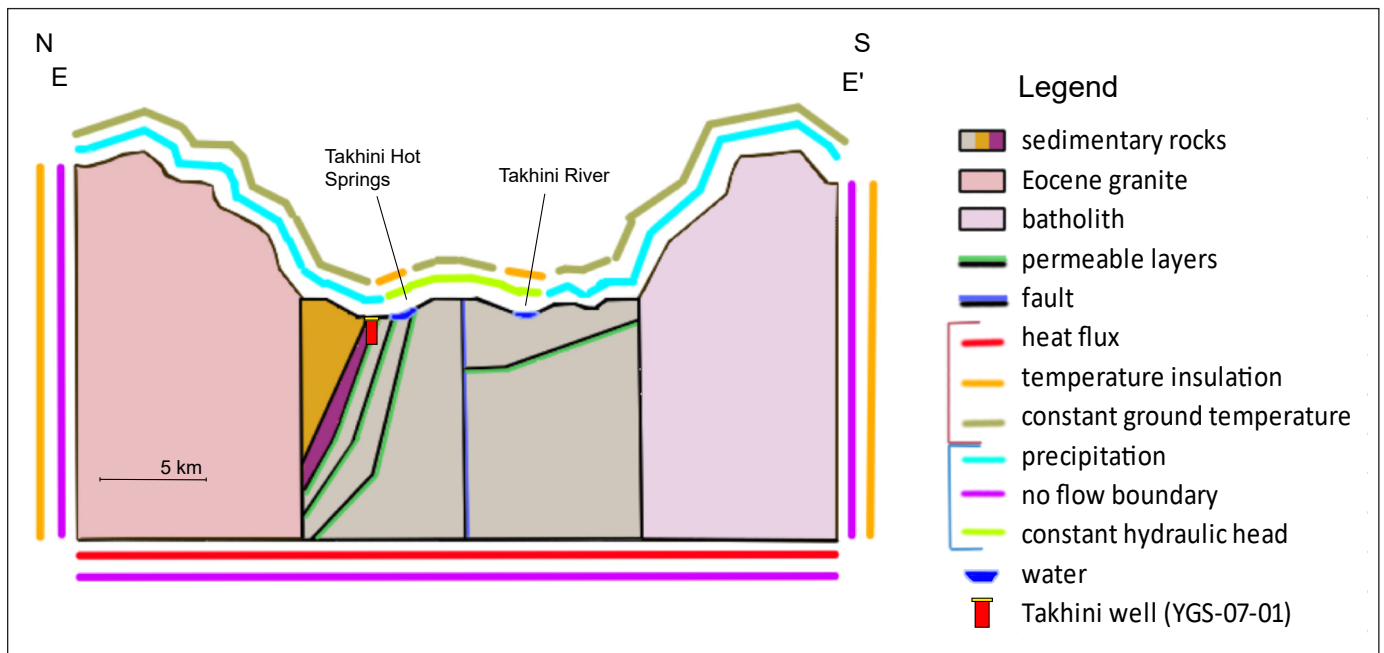
### Geometry

The modelled section, referred to as E–E', is 31 km long (Fig. 8) and 4 km deep (Fig. 7). The model was chosen to incorporate the regional valleys and topographic highs and includes both the location of the Takhini Hot Springs and the projected Takhini well. The model also includes the subvertical normal fault that was mapped approximately 2 km east of the hot springs (projected

to the south of the hot springs in our model). The dimensions of the pluton and dip of the sedimentary units follow the interpretation of Langevin et al. (2020a, cross section A–A'; Fig. 3). The Flat Creek pluton occupies the northern 8.9 km of our model, whereas the Annie Ned batholith fills the southern part of the model, from 21.6 to 31 km. Sedimentary units dip at approximately 50 degrees to the north. The thickness and geometry of sedimentary units were mostly determined by trial and error, until simulations showed an appropriate well temperature profile and hot springs temperature. A 1D observation line was set approximately 2 km north of the hot springs, at the location of Takhini well, to evaluate temperature at depth. Sedimentary units and granitic rocks were defined as low-permeability 2D units. Faults and permeable layers are defined as 1D linear elements superimposed onto the 2D porous medium. The model geometry allowed the fluid to travel along faults and permeable layers.

### Hydrothermal properties and radioactive heat generation

All model input parameters for rock and fault properties are shown in Figure 7 and Table 1. The geology was simplified in the model to facilitate numerical development and computations, especially in sedimentary units. Geo1 and Geo2 represent the most



**Figure 7.** Conceptual model of the Takhini Hot Springs. BC: boundary condition.

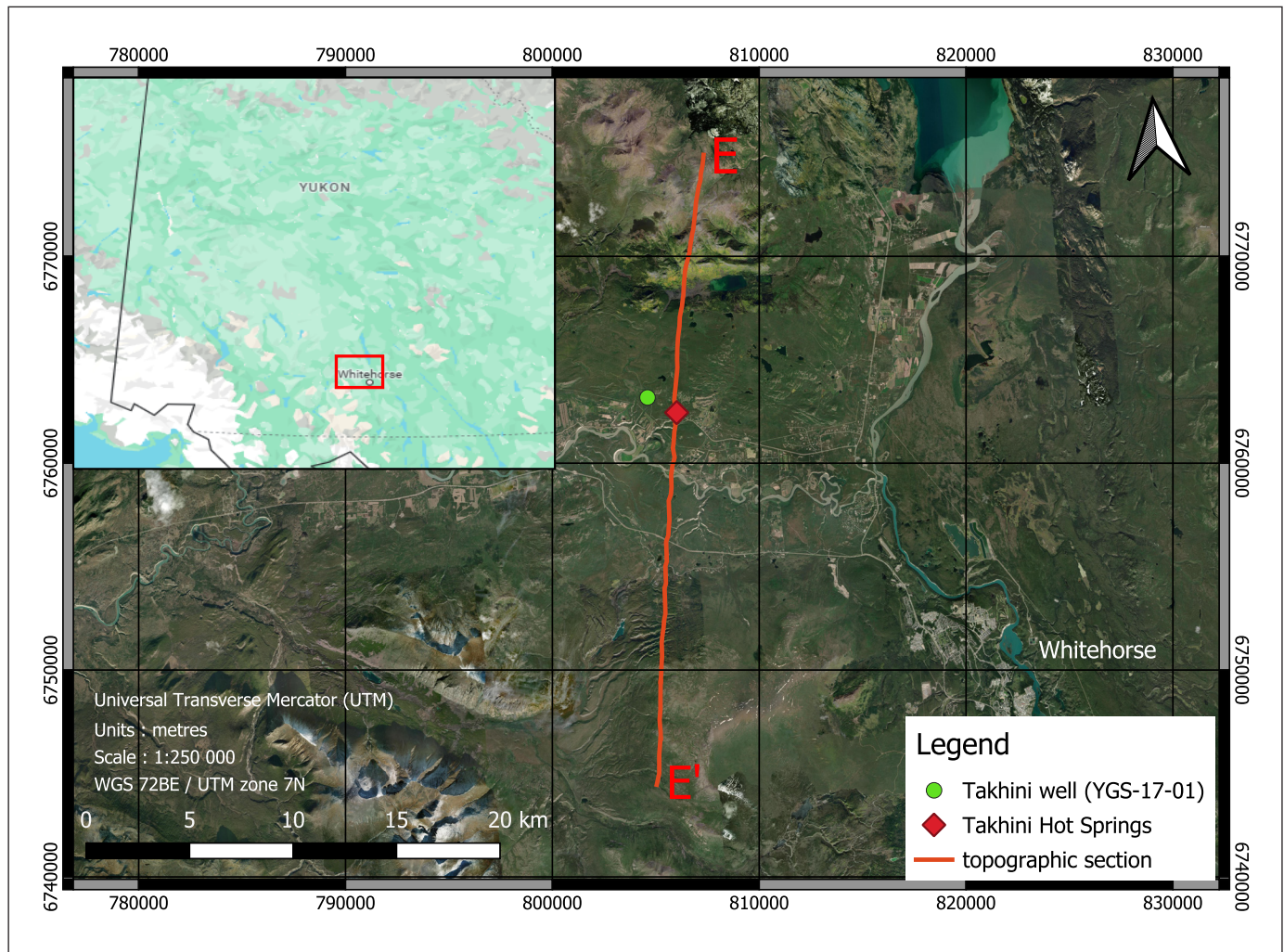


Figure 8. Location of topographic section E–E', used to define the surface of the model (Esri Canada, 2023).

common sedimentary rock types, namely deformed sandstone and volcanoclastic sandstone, respectively. All properties were assumed constant and not variable with depth.

Thermal conductivity and permeability for the fault and permeable layer were initially based on the work of Langevin et al. (2020a) from the analysis of two fault breccia samples that resulted in an average thermal conductivity of 0.98 W/(m·K) and an average hydraulic conductivity of  $7.05 \times 10^{-4}$  m/s. Although our initial model was based on these values, both properties changed when calibrating the model to reproduce the Takhini well temperature profile. High permeability was attributed to the permeable layers to create corridors ensuring water circulation. The calibrated model properties are listed in Table 1.

## Boundary conditions

### Flow

A surface constant hydraulic head of 640 m was applied to the whole valley, including both the river and the hot springs, to allow groundwater to exit through Takhini Hot Springs and the Takhini River. An infiltration rate of 18 mm/year was assigned to the surface boundary outside of the valley bottom, which is equal to approximately 7% of annual precipitation in the Whitehorse area (262 mm/year; Government of Canada, 2023). Water recharge diverges from annual precipitation because it specifically reflects the portion of precipitation that infiltrates the ground to replenish aquifers, accounting for factors like evapotranspiration and surface runoff. The recharge specified here is thought to be characteristic of deep aquifers. Regional groundwater flow is simulated and superficial aquifers

**Table 1.** Model input parameters for rock and fault properties in the Takhini Hot Springs area. Colours match those in Figure 5.

| Material        | Permeability (m <sup>2</sup> ) | Thermal conductivity of solids (W/(m·K)) | Porosity | Radiogenic heat generation (μW/m <sup>3</sup> ) | Thickness (m) |
|-----------------|--------------------------------|--|----------|---|---------------|
| Eocene granite  | 3.05 × 10 <sup>-15</sup>       | 2.5*                                     | 0.016    | 6.00**  | –             |
| batholith       | 9.78 × 10 <sup>-15</sup>       | 2.4*                                     | 0.016    | 1.66*   | –             |
| Geo1            | 2.00 × 10 <sup>-14</sup>       | 5  | 0.016    | 0   | –             |
| Geo2            | 2.37 × 10 <sup>-13</sup>       | 2.3                                      | 0.016    | 0   | –             |
| shale           | 8.00 × 10 <sup>-18</sup>       | 0.4                                      | 0.016    | 0   | –             |
| permeable layer | 7.00 × 10 <sup>-7</sup>        | 0.6                                      | 0.2      | 0   | 0.05          |
| fault           | 2.75 × 10 <sup>-8</sup>        | 0.6                                      | 0.1      | 0   | 0.01          |

\* from Langevin et al. (2020b); \*\* from Colpron et al. (2019)

that could be found in Quaternary deposits are not represented in the model. The left, right and bottom boundaries are impermeable (Fig. 7) allowing for groundwater flow to follow the natural topography with recharge in mountains and discharge in the valley.

### Heat transfer

Bottom heat flux was set to 0.05 W/m<sup>2</sup>, based on heat flow values in the area (Witter et al., 2018) and then adjusted by trial and error. Surface ground temperature was set according to equation 3:

$$T(K) = 278.15 - 0.0065 \times (z - 830) \quad (3)$$

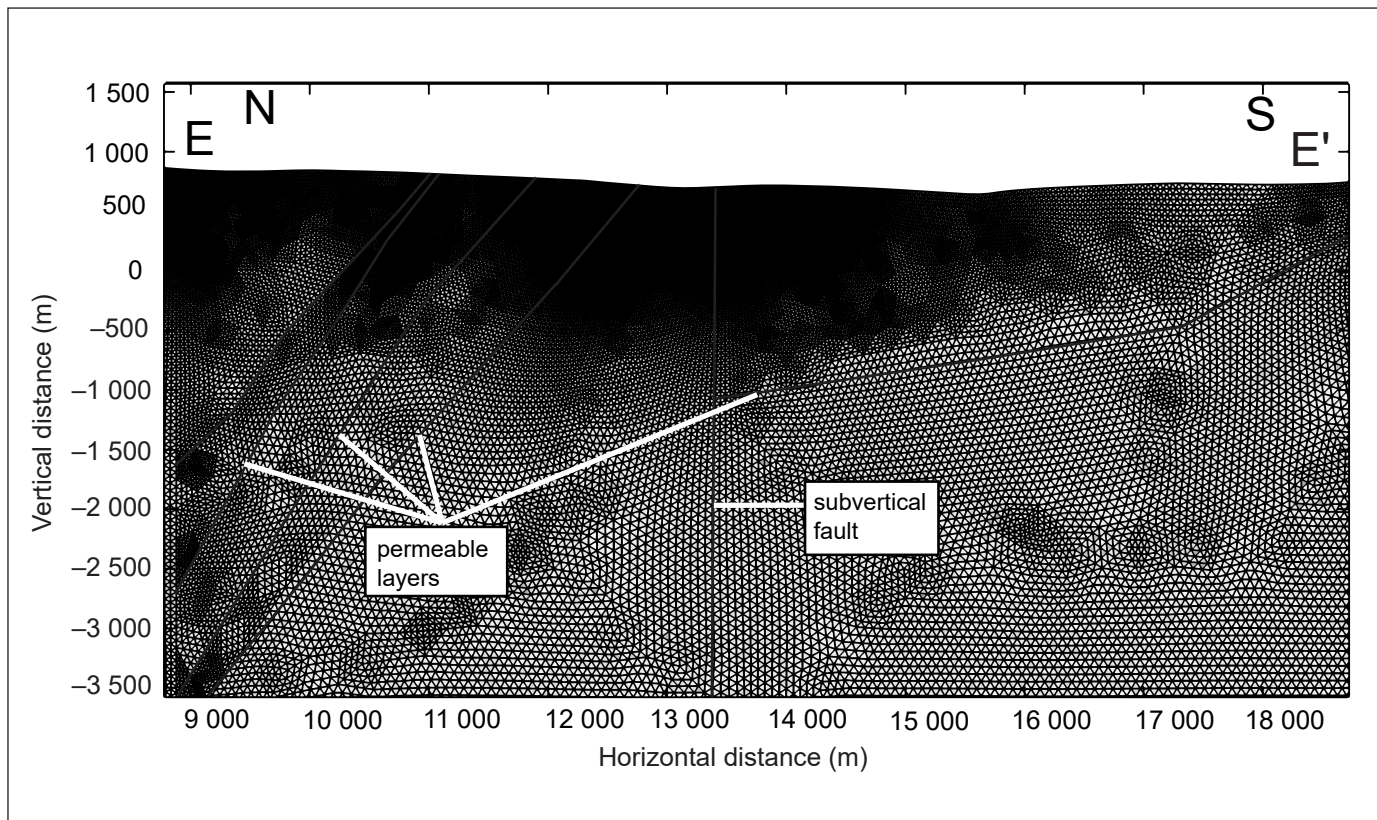
where  $z$  represents the elevation of every point on the upper boundary, in metres. The equation assumes a constant surface ground temperature of 278.15 K at an altitude of 830 m, with a temperature gradient of -0.0065 K/m to simulate lower temperatures at higher elevation. The surface ground temperature equation was applied on the whole upper boundary, except for the Takhini Hot Springs and the Takhini River, which are insulated boundaries where temperature is calculated according to the model solution.

### Mesh

A mesh is a computational grid or network of interconnected elements used to discretize and represent the geometry of a domain for numerical simulations. Refinement of the mesh increases from bottom to top and close to the faults and contacts to avoid convergence problems (Fig. 9). Groundwater flow mostly follows permeable layers, highlighting the importance of refining the surroundings of permeable layers to allow for accurate computations. The mesh is composed of extremely fine free triangles applied on the entire geometry and consists of 143 280 elements. The average skewness of the mesh is 0.8948, meaning that the mesh elements have shapes closer to their ideal configurations, contributing to improved numerical stability and reliability of the simulations.

### Sensitivity analysis

A sensitivity analysis was conducted once input parameters were adjusted to reproduce the Takhini well temperature profile and the temperature of Takhini Hot Springs. This calibrated model, where input parameters are adjusted to reproduce the observed temperature, is the base case scenario used as the foundation for



**Figure 9.** Finite element mesh of the 2D numerical model for the Takhini Hot Springs area.

subsequent simulations of the sensitivity analysis. The goal was to define the impact of each parameter on the simulated hot springs temperature and the temperature profile in the Takhini well. For every parameter, hot springs temperature and a well temperature profile was calculated and compared with the base case scenario. The parameters were grouped into three categories: material properties (red), model geometry (green) and boundary conditions (blue). Ultimately, thermal conductivity, permeability, radiogenic heat production, thickness of fractures, dip of layers, presence of a subvertical fault, recharge and heat flux were varied (Table 2).

## Results

### Temperature distribution and flow velocity

Figures 10 and 11 show temperature distribution with flow velocity vectors and hydraulic head distribution obtained with the calibrated model, respectively. Most of the groundwater on the north side of the model

travels through the permeable layers. Heat accumulates in the sedimentary units below the shale layer and near the hot springs. In comparison, the ground below the Takhini River, located to the south of the subvertical fault, is not as hot as the north side of the fault due to its distance (approximately 3 km) from the inclined permeable layers.

### Well temperature profile

The Takhini well temperature profile reported by Fraser *et al.* (2019) is compared to the simulated Takhini well temperature for the base case scenario in which parameters were adjusted to fit observations (Fig. 12). The simulated temperature gradient in the upper portion of the well shows a linear trend. This is due to the simplified model units and geometry used to save computational time. Local variations in the temperature gradient are not reproduced, though the effect of the permeable layer is clearly seen at the base of the well, where there is a steep change in temperature gradient.

**Table 2.** Model parameters that were varied for sensitivity analysis.

|                     | Parameter                                       | Units             | Initial value                                 | Variation                                      |
|---------------------|---|-------------------|---|--|
| material properties | thermal conductivity (Geo1 / Geo2)              | W/(m·K)           | 5 / 2.3                                       | ± 1  |
|                     | permeability (Geo1/Geo2)                        | m <sup>2</sup>    | 2.4e-14 / 2.37e-13                            | ÷ 100, × 100                                   |
|                     | radiogenic heat generation (Flat Creek / Annie) | µW/m <sup>3</sup> | 6 / 1.66                                      | ± 50%  |
| model geometry      | thickness of fractures                          | m                 | 0.05  | ÷ 10, × 10                                     |
|                     | angle of layers                                 | degrees           | 50  | ± 25   |
|                     | presence of a subvertical fault                 | –                 | –   | –  |
| boundary conditions | recharge  | mm/year           | 18 (6.87% of Whitehorse annual precipitation) | ± 13 (± 5% of Whitehorse annual precipitation) |
|                     | heat flux                                       | W/m <sup>2</sup>  | 0.05  | ± 0.015  |

## Sensitivity analysis

### *Takhini well temperature profile*

The simulated temperatures for the 500 m well are presented in Figure 13, showing the impact of individual parameters on ground temperature compared to the base case scenario. The sum of squared differences between temperature profiles with respect to that of the base case was calculated for all variations in parameters in the sensitivity analysis (Table 3).

The ranking of parameter impact (high to low) on the Takhini well temperature profile is as follows: 1) steeply dipping permeable layers, 2) recharge, 3) heat flux, 4) rock thermal conductivity, 5) rock permeability, 6) radiogenic heat generation, 7) thickness of permeable layers, 8) shallow-dipping permeable layers and 9) the presence of a subvertical fault at the centre of the model. Results indicate that both recharge and heat flux (boundary conditions) significantly influence the overall temperature of the model; rock thermal conductivity (input parameter) is also a notable factor.

Steeply dipping permeable layers reduce the overall temperature in the model, whereas the shallow-dipping model exhibits a profile similar to the base case scenario. Increasing rock permeability has more impact than decreasing it.

### *Takhini Hot Springs temperature*

The range of simulated hot springs temperature for all parameters is shown in Figure 14. The ranking of parameter impact (high to low) on the hot springs temperature is 1) heat flux, 2) rock thermal conductivity, 3) permeability, 4) recharge, 5) radiogenic heat generation, 6) thickness of permeable layers, 7) angle of permeable layers and 8) the presence of a sub-vertical fault. Results indicate that heat flux and recharge (boundary conditions), rock thermal conductivity and rock permeability (input parameters) significantly influence the hot springs temperature, whereas other parameters barely affect the water temperature. Increasing or reducing a single parameter would be sufficient to obtain a temperature of 46.5°C.

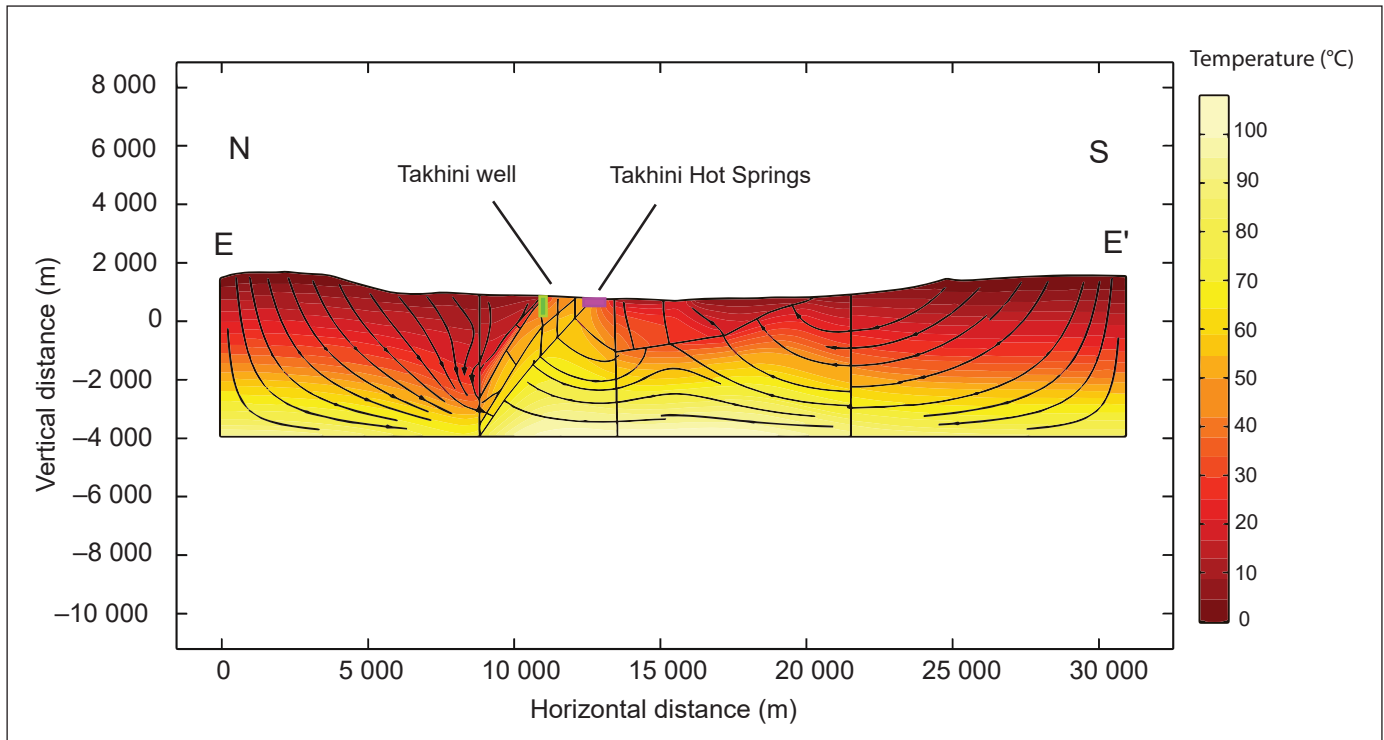


Figure 10. Simulated temperature distribution and flow lines for topographic section E-E' in the Takhini Hot Springs area.

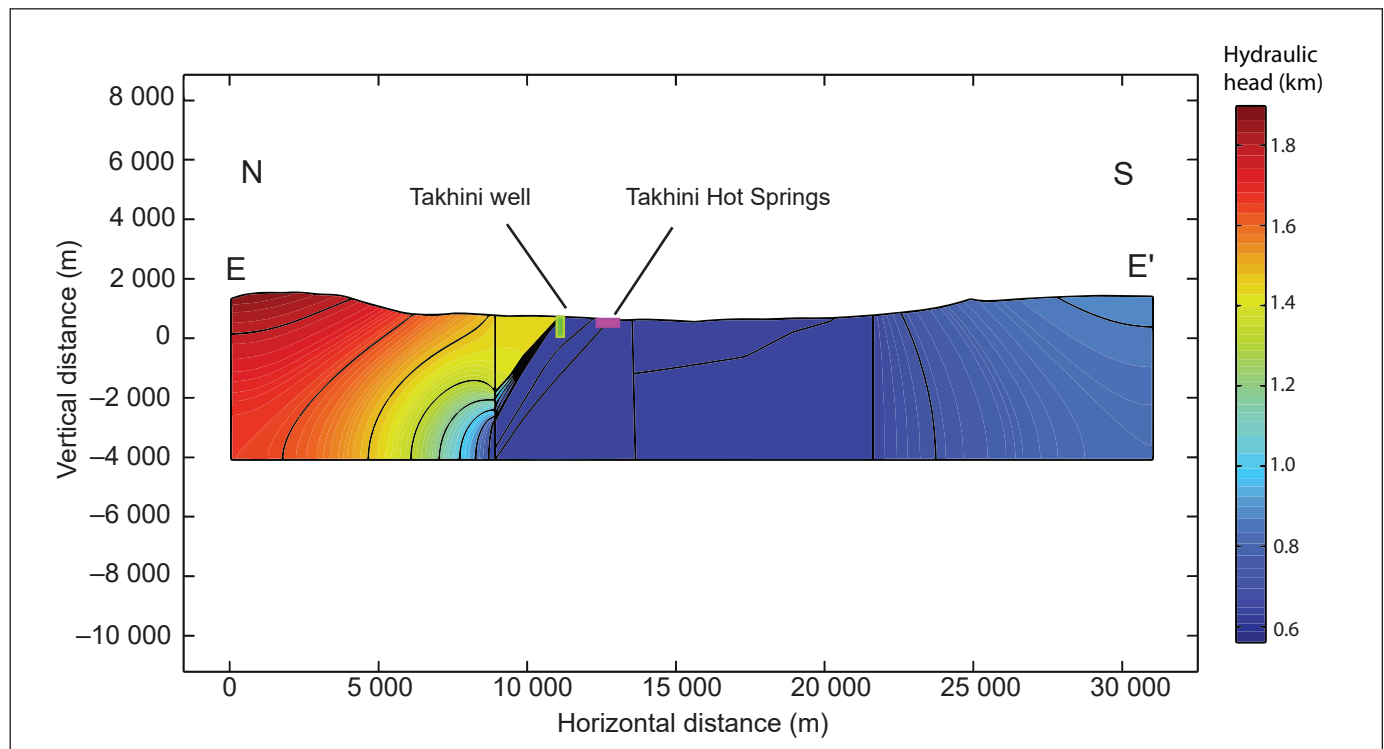
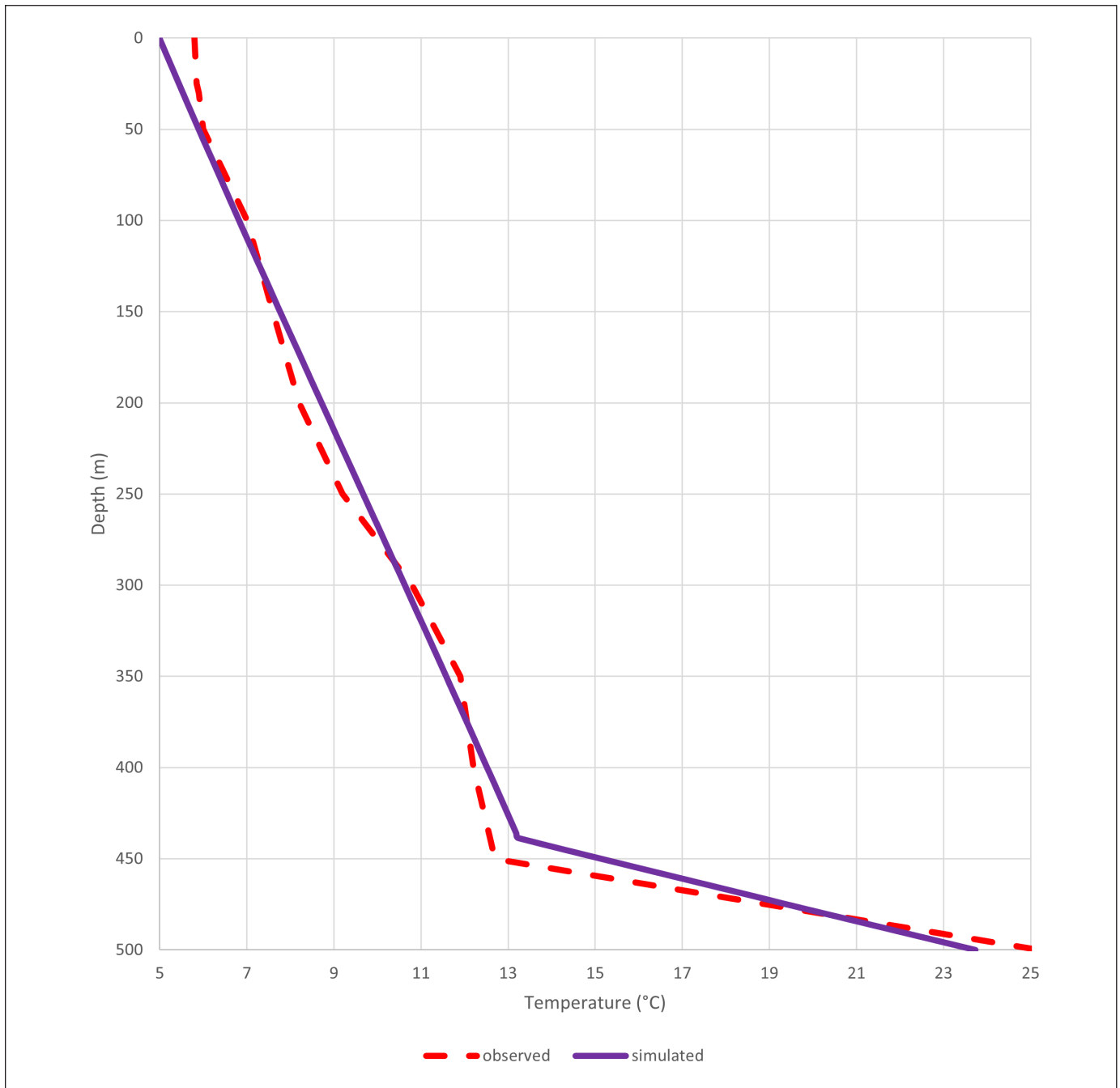


Figure 11. Simulated hydraulic head for topographic section E-E' in the Takhini Hot Springs area.



**Figure 12.** Comparison of observed (Fraser et al., 2019) and simulated (this study) temperature in the Takhini well (YGS-17-01) for the base case scenario.

## Discussion

Critical parameters such as heat flux, recharge, and rock thermal conductivity and permeability have substantial influence in our model of the Takhini Hot Springs geothermal system. These parameters mainly control the temperature's behaviour and dictate the overall thermal dynamics at the well and the hot springs'

locations. Heat flux and recharge influence the system's energy input and output, which have an important impact on the overall water temperature. Rock thermal conductivity and permeability are the main controllers of heat transfer and fluid flow, shaping the temperature distribution and the paths taken by the groundwater.

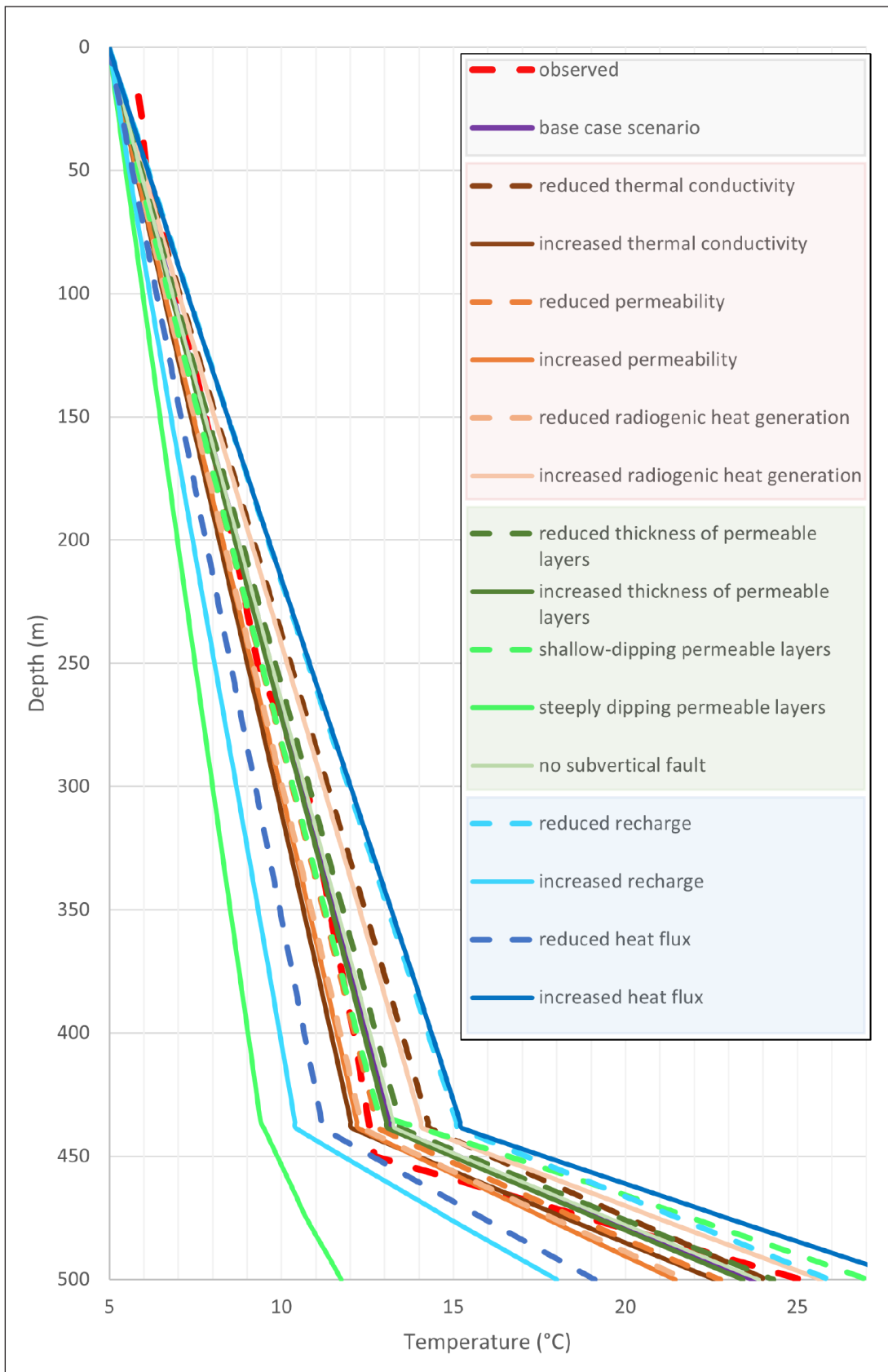


Figure 13. Simulated well temperature profiles for all parameters of the sensitivity analysis.



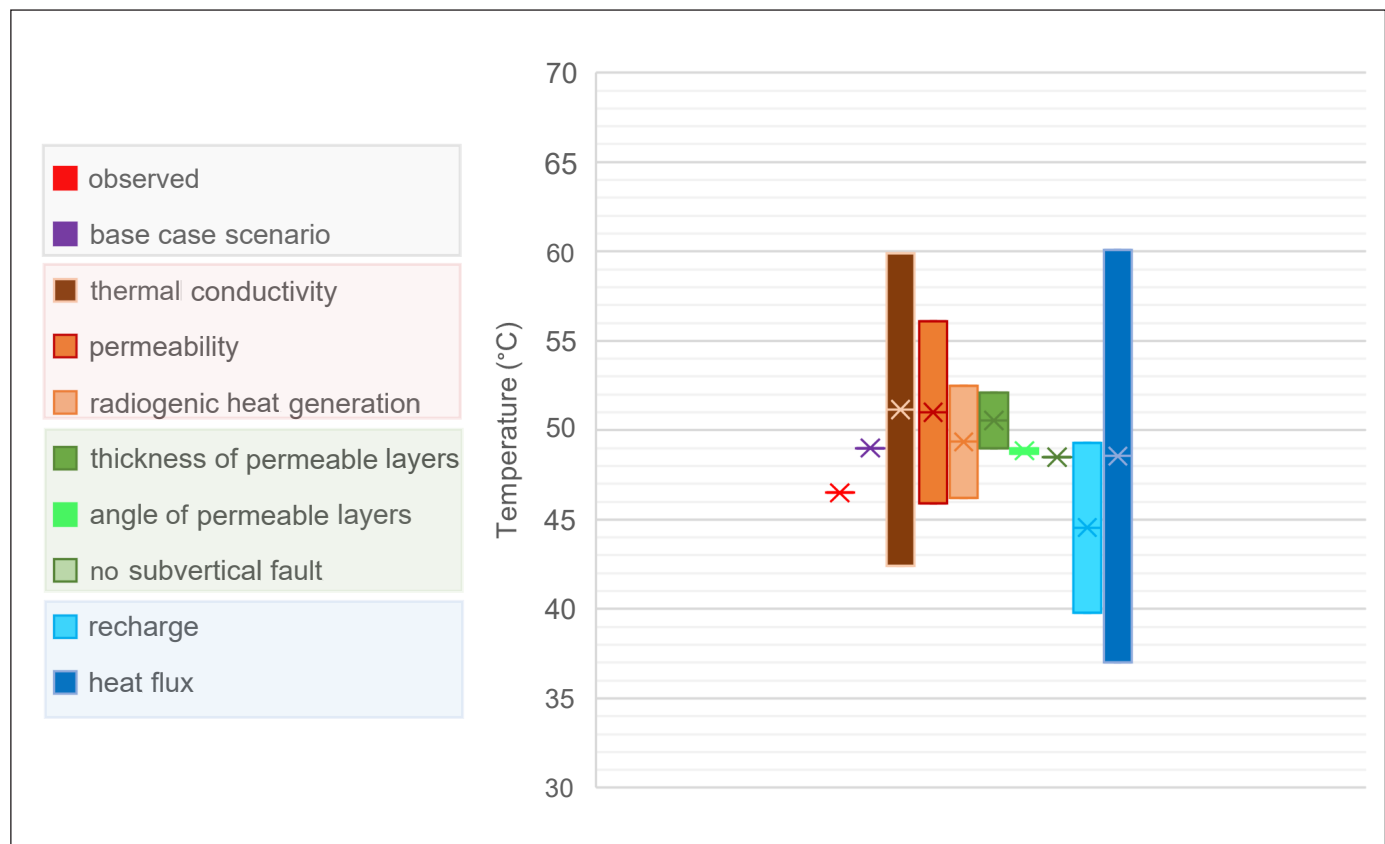
**Table 3.** Sum of squared differences for all scenarios with varying parameters of the sensitivity analysis. All parameters are compared to the base case scenario. Positive values imply an overall increase in the temperature profile, whereas negative values suggest a decrease in temperature..

| Parameter                            | Sum of squared difference |
|--------------------------------------|---------------------------|
| reduced thermal conductivity         | 15.24                     |
| increased thermal conductivity       | -21.02                    |
| reduced permeability                 | -4.80                     |
| increased permeability               | -22.70                    |
| reduced radiogenic heat generation   | -17.89                    |
| increased radiogenic heat generation | 17.89                     |
| reduced fractures thickness          | 1.59                      |
| increased fractures thickness        | -0.43                     |
| shallow-dipping beds                 | -27.44                    |
| steeply dipping beds                 | -466.81                   |
| no subvertical fault                 | 0.11                      |
| reduced recharge                     | 60.75                     |
| increased recharge                   | -172.47                   |
| reduced heat flux                    | -96.85                    |
| increased heat flux                  | 96.85                     |

The model shows that groundwater seepage toward the surface can be caused by highly permeable layers of inclined sedimentary rocks. This results in high temperature in the Takhini Hot Springs area, allowing the hot water to circulate freely. It also shows the importance of low-permeability layers (shale), which tend to act as an insulator to the underlying reservoir. The steeply and shallowly dipping permeable layers exhibit distinct differences in their flow path. This geometric variation poses a challenge when attempting to evaluate its impact compared to that of other parameters; however, it is possible to adjust the geometry so that the observed temperature profile can be reproduced. The simulated well temperature reveals that shallow-dipping permeable layers allow a better circulation of the water from the surrounding mountains to the bottom of the valley, with hot water circulation along this path. Such geological settings are, therefore, more likely to create the high temperature gradient measured at the base of the Takhini well. Subvertical permeable layers do not significantly impact water circulation in the Takhini Hot Springs area but allow deeper and hotter water to directly reach the surface. The dip of the permeable layers in the model is opposite to the groundwater flow direction, creating a significant hydraulic head difference from the bottom to the top of the layers and allowing groundwater to rise.

The model geometry and input parameters are based on geological characteristics of the Takhini Hot Springs area. Calibrations based on field measurements, such as the Takhini well temperature profile and actual hot springs water temperature, ensure that the model is grounded in empirical data and not just based on theoretical inputs. The alignment between the simulations and field observations emphasizes the reliability of the model's predictions. The sensitivity analysis, which involved varying key parameters, highlighted model uncertainty that could be reduced with additional field observations.

This study provides new knowledge that can assist geothermal exploration in the Whitehorse trough. The identification of critical parameters, such as heat flux, recharge, and rock thermal and hydraulic conductivity—and their impact on the hydrothermal system—can provide guidelines for geothermal exploration. We believe that hot water circulation is caused by permeable layers in sedimentary units intercepting regional groundwater flow. Identifying



**Figure 14.** Simulated and observed (Fraser et al., 2019) temperatures at Takhini Hot Springs.

the pathways for fluid movement can help predict temperature gradients, as well as identify new targets in similar regions characterized by inclined sedimentary units that dip away from regional groundwater flow, as observed on the north side of the model. These areas can exhibit a favourable hydraulic head contrast between the base and top of the sedimentary layers, facilitating an efficient upward flow of hot water. Other locations in the Whitehorse trough could have similar characteristics, although few springs are observed at surface.

The simplified model facilitated our understanding of the flow and heat transfer mechanisms influencing the temperature distribution in the Takhini Hot Springs geothermal system. The thermal conductivity and permeability were assumed to be uniform for all units and they did not evolve with increasing temperature and pressure. This simplification favours convection over conduction. Having well data from only a single location is an important limitation in our study. Better knowledge of the dip angle, thickness and

fracture density of sedimentary units would allow a better representation of the geological model. It is difficult to identify a single rock type responsible for transporting water to surface because the model is based on simplified geology. We also simplified the basin lateral boundaries with straight vertical margins for both plutons, which differs from the hydrothermal interpretation of Langevin et al. (2020a). The overall geometry is, therefore, not an accurate representation of the Takhini Hot Springs area, but it gives a general idea of its shape and hydrothermal interactions. Previous studies indicated that the Whitehorse area has a moderate heat flux, reaching up to 60 mW/(m<sup>2</sup>) (Grasby et al., 2012; Witter et al., 2018), which affected the temperature distribution of the entire model. A thicker pluton with higher concentrations of radiogenic elements could contribute significantly to the overall radiogenic heat generation, whereas a higher heat flux enhances the rate of heat production. Although the heat flux at the base of the model and the internal heat generation rate of plutons are likely linked, the depth of our model is insufficient for confirmation. To assess

the relationship between these factors and determine whether surrounding intrusions could represent heat sources, a deeper model that includes information on pluton thickness is required.

## Conclusions

Our 2D groundwater flow and heat transfer model of the Takhini Hot Springs area was used to explore the role of key parameters—heat flux, recharge, and rock thermal conductivity and permeability—in defining the thermal dynamics of the Takhini Hot Springs geothermal system. These factors strongly affect flow and heat transfer in the basin, influencing both the simulated well and the hot springs temperatures. The model emphasizes the importance of permeable layers that facilitate hot water circulation below a low-permeability shale layer acting as an insulator to the underlying geothermal reservoir.

Built from field observations, the model is empirical and offers a good degree of accuracy, validated through calibration and a sensitivity analysis on various parameters. The study proposes a comprehensive understanding of the influence of the geometry of sedimentary units and interaction of surrounding plutons on hydrothermal flow. Although our model offers a better understanding of the Takhini Hot Springs geothermal system, it is limited by simplifications involving uniform unit properties and relying on an interpreted geological cross section. Geophysical surveys to image geological structures at depth and infer rock properties could help better constrain the model. Nevertheless, the study contributes to the understanding of Takhini Hot Springs, providing practical guidelines for exploring geothermal resources in the Whitehorse trough and beyond, and contributes to the Government of Yukon's larger initiative to identify green energy solutions.

## Acknowledgments

This work was funded under a research agreement from the Yukon Geological Survey and an Alliance Grant from the Natural Science and Engineering Research Council of Canada to the Institut national de la recherche scientifique. Special thanks to Tiffani Fraser and Maurice Colpron for their invaluable assistance in providing insightful advice for this paper.

## References

- Alvarado Blohm, F.J., Urzua, A., Ebel, J. and Kafka, A., 2016. Determination of hydraulic conductivities through grain-size analysis. MSc thesis, Boston College University, Chestnut Hill, United States, 102 p.
- Artemieva, I.M., Thybo, H., Jakobsen, K., Sørensen, N.K. and Nielsen, L.S.K., 2017. Heat production in granitic rocks: Global analysis based on a new data compilation GRANITE2017. *Earth Science Reviews*, vol. 172, p. 1–26. <https://doi.org/10.1016/j.earscirev.2017.07.003>
- Colpron, M., 2019. Potential radiogenic heat production from granitoid plutons in Yukon. Yukon Geological Survey, Open File 2019-16, 1 map and data.
- Colpron, M., Crowley, J.L., Gehrels, G.E., Long, D.G.F., Murphy, D.C., Beranek, L.P. and Bickerton, L., 2015. Birth of the northern Cordilleran orogen, as recorded by detrital zircons in Jurassic synorogenic strata and regional exhumation in Yukon. *Lithosphere*, vol. 7, no. 5, p. 541–562. <https://doi.org/10.1130/L451.1>
- Colpron, M., Sack, P.J., Crowley, J.L., Beranek, L.P. and Allan, M.M., 2022. Late Triassic to Jurassic magmatic and tectonic evolution of the Intermontane terranes in Yukon, northern Canadian Cordillera: Transition from arc to syn-collisional magmatism and post-collisional lithospheric delamination. *Tectonics*, vol. 41, no. 2, article e2021TC007060. <https://doi.org/10.1029/2021TC007060>.
- COMSOL, 2023. COMSOL Multiphysics, version 6.1, COMSOL AB, Stockholm, Sweden. <https://www.comsol.com/comsol-multiphysics> [accessed November 5, 2023]
- Core Lab Instruments, 2016. PPP-250 Portable probe permeameter operations manual. Core Lab Instruments. Tulsa, United States, 6 p.
- Esri Canada, 2023. Satellite Image of Yukon, scale 1:250 000, ESRI, Redlands.

- Fraser, T., Colpron, M. and Relf, C., 2019. Evaluating geothermal potential in Yukon through temperature gradient drilling. In: Yukon Exploration and Geology 2018, K.E. MacFarlane (ed.), Yukon Geological Survey, p. 75–90.
- Gabrielse, H., Murphy, D.C. and Mortensen, J.K., 2006. Cretaceous and Cenozoic dextral orogeny parallel displacements, magmatism and paleogeography, north-central Canadian Cordillera. In: Paleogeography of the North American Cordillera: Evidence For and Against Large-Scale Displacements, J.W. Haggart, J.W.H. Monger and R.J. Enkin (eds.), Geological Association of Canada, Special Paper 46, p. 255–276.
- Government of Canada, 2023. Canadian Climate Normals 1981–2010 Station Data for Whitehorse. [https://climate.weather.gc.ca/climate\\_normals/results\\_1981\\_2010\\_e.html?searchType=stnName&txtStationName=whitehorse&searchMethod=contains&txtCentralLatMin=0&txtCentralLatSec=0&txtCentralLongMin=0&txtCentralLongSec=0&stnID=1617&dispBack=0](https://climate.weather.gc.ca/climate_normals/results_1981_2010_e.html?searchType=stnName&txtStationName=whitehorse&searchMethod=contains&txtCentralLatMin=0&txtCentralLatSec=0&txtCentralLongMin=0&txtCentralLongSec=0&stnID=1617&dispBack=0) [accessed June 19, 2023]
- Government of Yukon, 2022. Our Clean Future: 2021 Annual Report. Government of Yukon, Whitehorse, Canada, 82 p. <https://our-clean-future.service.yukon.ca/sites/default/files/2023-10/env-our-clean-future-2021-annual-report.pdf>
- Grasby, S.E., Jessop, A., Kelman, M., Ko, M., Chen, Z., Allen, D.M., Bell, S., Ferguson, G., Majorowicz, J., Moore, M., Raymond, J. and Therrien, R., 2012. Geothermal energy resource potential of Canada. Geological Survey of Canada, Open File 6914, 322 p., <https://doi.org/10.4095/291488>.
- Hart, C.J.R., 1997. A transect across northern Stikinia: Geology of the northern Whitehorse map area, southern Yukon Territory (105D/13-16). Exploration and Geological Services Division, Yukon, Indian and Northern Affairs Canada, Bulletin 8, 112 p.
- Langevin, H., Fraser, T. and Raymond J., 2020a. Assessment of thermo-hydraulic properties of rock samples near Takhini Hot Springs, Yukon. In: Yukon Exploration and Geology 2019, K.E. MacFarlane (ed.), Yukon Geological Survey, p. 57–73.
- Langevin, H., Fraser, T.A. and Raymond, J., 2020b. Assessment of the thermo-hydraulic properties of rock samples near Takhini Hot Springs and in the Tintina fault zone, Yukon. Yukon Geological Survey, Miscellaneous Report 19, 30 p.
- Moeck, I.S., 2014. Catalog of geothermal play types based on geologic controls. *Renewable and Sustainable Energy Reviews*, vol. 37, p. 867–882. <https://doi.org/10.1016/j.rser.2014.05.032>
- Monger, J.W.H. and Price, R.A., 2002. The Canadian Cordillera: Geology and tectonic evolution. *Canadian Society of Exploration Geophysicists Recorder*, vol. 27, p. 17–36.
- van Drecht, L.H., Beranek, L.P., Colpron, M. and Wiest, A.C., 2022. Development of the Whitehorse trough as a strike-slip basin during Early to Middle Jurassic arc-continent collision in the Canadian Cordillera. *Geosphere*, vol. 18, no. 5, p. 1538–1562. <https://doi.org/10.1130/GES02510.1>.
- Witherspoon, P.A., Wang, J.S.Y., Iwai, K. and Gale, J.E., 1980. Validity of Cubic law for fluid flow in a deformable rock fracture. *Water Resources Research*, vol. 16, issue 6, p. 1016–1024. <https://doi.org/10.1029/WR016i006p01016>.
- Witter J.B., Miller C.A., Friend, M. and Colpron, M., 2018. Curie point depths and heat production in Yukon, Canada. *Proceedings, 43<sup>rd</sup> Workshop on Geothermal Reservoir Engineering*, Stanford University, Stanford, California, February 12–14, 2018, 11 p.
- Yukon Geological Survey, 2022. Yukon digital bedrock geology. Yukon Geological Survey, <https://data.geology.gov.yk.ca/Compilation/3>, [accessed January 3, 2024]
- Yukon Geological Survey, 2023. Surficial geology dataset. Yukon Geological Survey, <https://data.geology.gov.yk.ca/Compilation/33>, [accessed January 3, 2024]